Seasonal and Internannual Variability of Estuarine Circulation in a Box Model of the Strait of Georgia and Juan de Fuca Strait

Ming Li, Ann Gargett and Ken Denman
Institute of Ocean Sciences, P.O. Box 6000
Sidney, B.C. V8L 4B2

[Original manuscript received 3 January 1998; in revised form 18 August 1998]

ABSTRACT *A box model of the Strait of Georgia and Juan de Fuca Strait, British Columbia, Canada is developed to investigate the estuarine circulation driven by Fraser River runoff but modulated by tidal mixing in Haro Strait which connects the two straits. The water mass exchange between the Juan de Fuca Strait and the Pacific Ocean is parametrized by a restoring salinity boundary condition. In addition to horizontal advection of water masses, the salinity in the lower layer of Juan de Fuca Strait is relaxed to the Pacific salinity. For realistic values of the fresh water flux and vertical eddy diffusivity, the model predicts a seasonal cycle of salinities and water mass transports in reasonable agreement with the observations. The salinity distribution in the estuary is determined by the combined effect of river runoff and vertical mixing. Tidal mixing in Haro Strait not only reduces stratification but also causes a spring-neap tidal modulation of salinities.*

Multi-year calculations show a rapid response of the estuarine circulation to interannual variability in the fresh water forcing and in the properties of the continental shelf water which enters the deep layer of the Juan de Fuca Strait. The salinities and volume fluxes adjust to the new river runoff within a year, consistent with observational estimates of a short flushing time in the estuary.

RÉSUMÉ *Un modèle "boîte" du détroit de Georgie et du détroit de Juan de Fuca, Colombie Britannique, Canada, a été construit afin d'étudier la circulation estuarienne imposée par l'écoulement du fleuve Fraser, modulé par le mélange dû aux marées dans le détroit de Haro qui relie les deux détroits. L'échange de masse d'eau entre le détroit de Juan de Fuca et l'océan Pacifique est paramétré au moyen d'une condition frontière qui rétablit la salinité. En plus de l'advection horizontale des masses d'eau, la salinité de la couche inférieure du détroit de Juan de Fuca est ramenée à la salinité du Pacifique. Pour des valeurs réalistes de l'écoulement d'eau fraîche et de la diffusion tourbillonnante verticale, le modèle prédit un cycle saisonnier de salinité et de transport de masse d'eau qui est en accord raisonnable avec les observations. La distribution de salinité dans l'estuaire est déterminée par l'effet combiné de l'écoulement du fleuve et du mélange vertical. Le mélange dû aux marées dans le détroit*

ATMOSPHERE-OCEAN 37 (1) 1999, 1–19 0705-5900/99/0000-0001$1.25/0

de Haro réduit non seulement la stratification, mais provoque aussi une modulation bimensuelle de la salinité de la marée.

Des calculs sur plusieurs années montrent une réponse rapide de la circulation estuarienne à la variabilité interannuelle du forçage par l'eau fraîche ainsi qu'aux propriétés de l'eau du plateau continental qui pénètre dans la couche profonde du détroit de Juan de Fuca. La salinité et le volume des écoulements s'adaptent à l'écoulement du fleuve en moins d'un an, en accord avec l'hypothèse, basée sur les observations, d'un court temps de chasse de l'estuaire.

1 Introduction

The Strait of Georgia and Juan de Fuca Strait are two connected coastal ocean basins situated between Vancouver Island and the mainland coasts of British Columbia and Washington State (Fig. 1). A primary forcing of this system is the fresh water runoff from the Fraser River, which peaks during the summer freshet. A plume of brackish, silt-laden water is often seen to spread over the oceanic water in the southern part of the Strait of Georgia. The estuarine flow is characterized by a seaward outflow in the upper portion of the water column and a landward inflow below. The net seaward flow of brackish surface water depends on the amount of fresh water entering the system and the degree of entrainment of deep saline water into the surface layer.

The Strait of Georgia is connected to Juan de Fuca Strait mainly through the channel of Haro Strait and to a lesser extent through the narrower Rosario Strait. Strong tidal mixing occurs in Haro Strait. The first mixing region encountered by the estuarine outflow is known as Boundary Passage, a sinuous channel whose sill does not extend completely across the pass. Further mixing occurs at a second sill 75 km seaward of Boundary Pass, at the eastern end of Juan de Fuca Strait. The tidal mixing in Haro Strait plays an important role in the seaward export of fresh water and the landward import of deep return flow. Griffin and LeBlond (1990) suggested that, during neap tides, reduced tidal mixing allows an enhanced flow of low salinity surface waters seawards through Boundary Passage. Enhanced inflow of deep saline water also appears to occur during the neap tides when dense gravity currents spill over the sill at depth (Le Blond et al., 1991).

Juan de Fuca Strait is a weakly-stratified estuary with strong tidal currents. Current meter measurements suggested that the estuary consists of a two-layer circulation with a net outflow in the upper 75- to 125-m depth range and net inflow beneath. The upper and lower layer volume flow rates are nearly equal in magnitude, ranging from 90 to 160 $\times$ 10^3 m^3 s^{-1} (Thomson, 1994). The salt and volume budgets are balanced by the relatively small difference between the outflow and inflow rates. From historical data, Ott and Garrett (1998) estimated a maximum vertical eddy viscosity of 0.03 m^2 s^{-1}, suggesting that turbulence or cross-channel secondary circulation may produce strong vertical mixing in local regions of this strait.

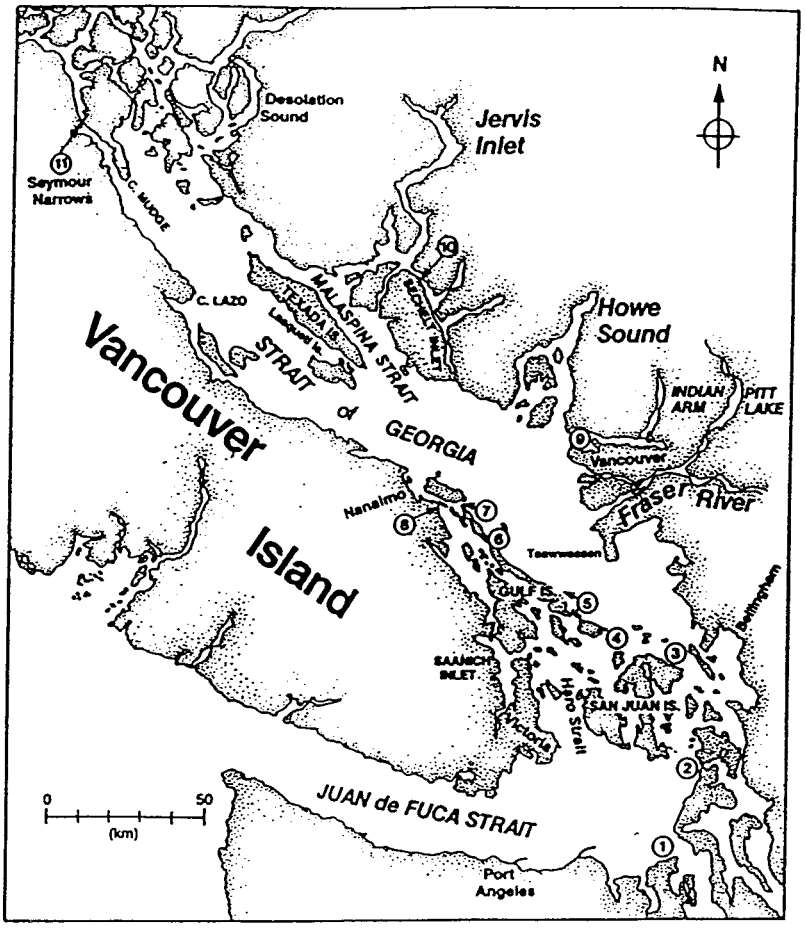

Fig. 1 A map of Strait of Georgia and Juan de Fuca Strait. The two basins are connected through the narrow channel of Haro Strait where tidal mixing is vigorous. Fresh water from the Fraser River is released into the Strait of Georgia, driving a two-layer estuarine circulation. The Puget Sound drainage basin (not shown) is connected to Juan de Fuca Strait through channels labelled 1.

The Georgia-Fuca estuary is linked to the Pacific Ocean mainly through the broad reaches of Juan de Fuca Strait and to a lesser extent through the narrow and constricted channels of Johnstone Strait in the north. From late spring to early fall, the North Pacific High pressure system generates winds predominantly from the north to northwest and produces upwelling of cold, high salinity and nutrient-rich water over the continental margin. From late fall to early spring, winds are predominantly from the southeast due to the Aleutian Low pressure system in the

Gulf of Alaska, leading to increased temperatures and lower salinities over the shelf (Thomson et al., 1989).

In this paper we develop a box model for the Georgia-Fuca system. Since the Strait of Georgia and Juan de Fuca Strait are semi-closed ocean basins, they are well suited to the box model. Our primary objective is to understand seasonal and interannual variability of the estuarine circulation associated with fluctuations in the Fraser River runoff and in the properties of the continental shelf water in the North Pacific. Although more sophisticated three-dimensional tidal models have been developed for this region (Foreman et al., 1994; Crean et al., 1988), they are computation intensive and may not be suitable for long-term integrations. The model presented here, however, because of its simplicity and low demand on computer resources, can be run repeatedly over climate timescales (decades) to test sensitivities of the model. Box models have been used to investigate climate variability of thermohaline circulation in the deep ocean (e.g., Gargett and Ferron, 1996; Thual and McWilliams, 1992). It is our intention to apply a similar approach to estuarine circulation in a coastal environment. Our second motivation for developing a box model was to understand the factors controlling foodweb dynamics in the estuary, e.g., the estuarine circulation is the primary nutrient source for phytoplankton production (Mackas and Harrison, 1997). Given the complexity of a foodweb model, it seems sensible to couple it initially with a simple estuarine circulation model that incorporates key physical processes but allows many simulations to determine sensitivities to biological parameters. Results with the coupled biological model will be reported elsewhere.

In a recent paper, LeBlond et al. (1994) developed a box model to study surface salinity variations in the Juan de Fuca Strait. They focused on the export of fresh water and treated the lower layer as a stagnant layer having constant salinity. Our model, however, tracks the time evolution of the salinities of both surface and deep waters in the Georgia-Fuca estuary.

2 Model formulation

Figure 2a shows a schematic diagram of the box model for the Georgia-Fuca estuarine system. We divide this system into three basins: Georgia basin, Haro Strait (and Boundary Passage) and Fuca basin, each of which consists of an upper box and a lower box. Flows through the narrower Rosario Strait are much weaker than through Haro Strait and are thus neglected in this study. Since only a small percentage of fresh water leaves through Johnstone Strait (Thomson, 1994), we close the Georgia basin at the northern end. The main exchange between the estuary and the Pacific Ocean is at the western end of the Juan de Fuca Strait.

We denote the volumes of water by V_g, V_h and V_j in which the subscripts g, h and f represent the Georgia, Haro and Fuca basins. The corresponding surface areas are A_g, A_h and A_f. The upper box is denoted by subscript u and the lower box by subscript l. The thickness of the upper box is h_u and that of the lower box is h_l. We assume that $h_u = 50$ m and $h_l = 150$ m are the same across all three basins.

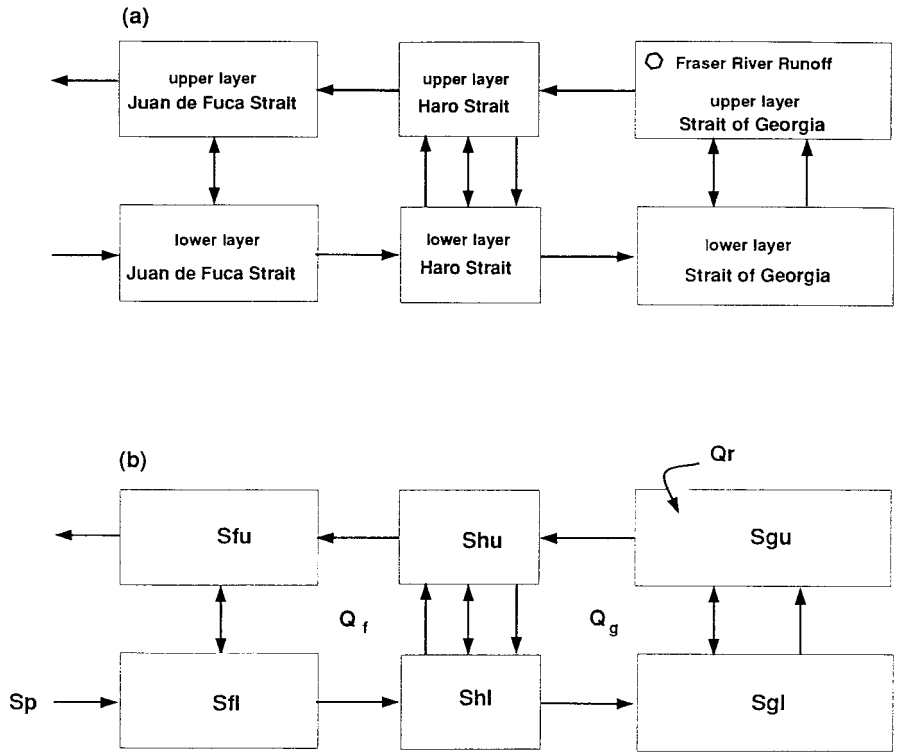

Fig. 2 (a) Schematic of a box model for the Georgia-Fuca estuary. We divide the estuary into Georgia, Haro and Fuca basins, each of which consists of an upper and a lower box. (b) Definition of symbol notation for salinity. Q_r represents the Fraser River runoff and S_p the Pacific salinity. Q_g is the volume flux between the Strait of Georgia and Haro Strait and Q_f the volume flux between Haro Strait and Juan de Fuca Strait.

Rough estimates show that $V_g \approx 800$ km^3, $V_h \approx 100$ km^3 and $V_f \approx 400$ km^3. The salinities in the six boxes are denoted by $\tilde{S}_{gu}$, $\tilde{S}_{gl}$, $\tilde{S}_{hu}$, $\tilde{S}_{hl}$, $\tilde{S}_{fu}$ and $\tilde{S}_{fl}$, the volume flux between Georgia and Haro basins by Q_g and that between Haro and Fuca basins by Q_f (Fig. 2b).

A primary forcing of the estuary is the runoff from the Fraser River. This fresh water flux Q_r varies seasonally from less than 10^3 m^3 s^{-1} in winter to more than 10^4 m^3 s^{-1} at the peak of the freshet in summer (Thomson, 1981). Q_r accounts for about 75% of the total fresh water input to the Strait of Georgia. Runoffs from small river tributaries and wintertime precipitation make a small contribution to the total fresh flux and are ignored.

To simulate the seasonal variation of Fraser River runoff, we choose

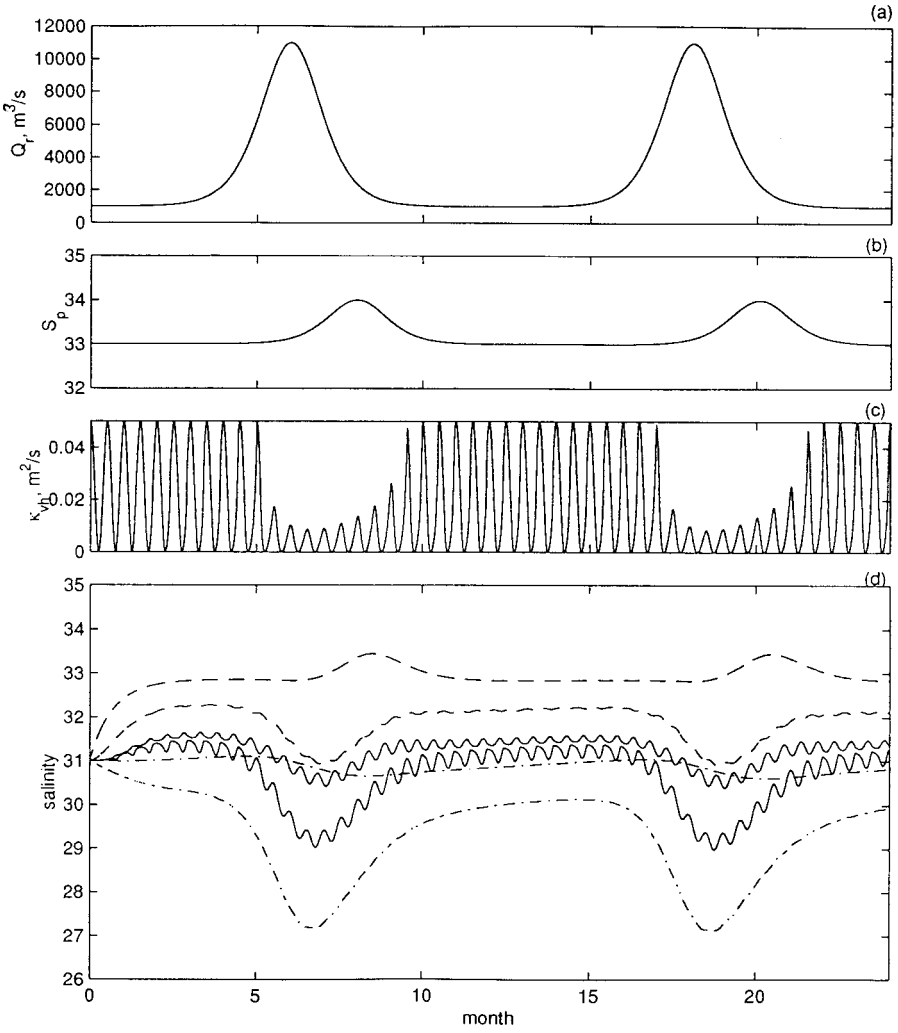

Fig. 3 A typical seasonal cycle of estuarine circulation. The first year is the model's start-up phase. (a) The Fraser River runoff Q_r. (b) Pacific salinity $\tilde{S}_p$. (c) Vertical eddy diffusivity corresponding to the spring-neap cycle of tidal mixing in Haro Strait. (d) Time series of salinities. Dot-dashed lines represent salinities in Georgia basin, solid lines in Haro Strait and dashed lines in Fuca basin. Larger values are salinities in the lower boxes. (e) Vertical stratification (salinity differences between the upper and lower boxes) in the Strait of Georgia (dot-dashed), Haro Strait (solid) and Juan de Fuca Strait (dashed). (f) Volume fluxes Q_g between Georgia and Haro basins (thick solid) and Q_f between Haro and Fuca basins (thin solid) where Q_f has been offset by 3 units for visual clarity. (g) Salinity flux, Q_{fr}, due to the Fraser River runoff (solid) and that, Q_{fp}, due to the exchange between Juan de Fuca Strait and the Pacific Ocean (dashed).

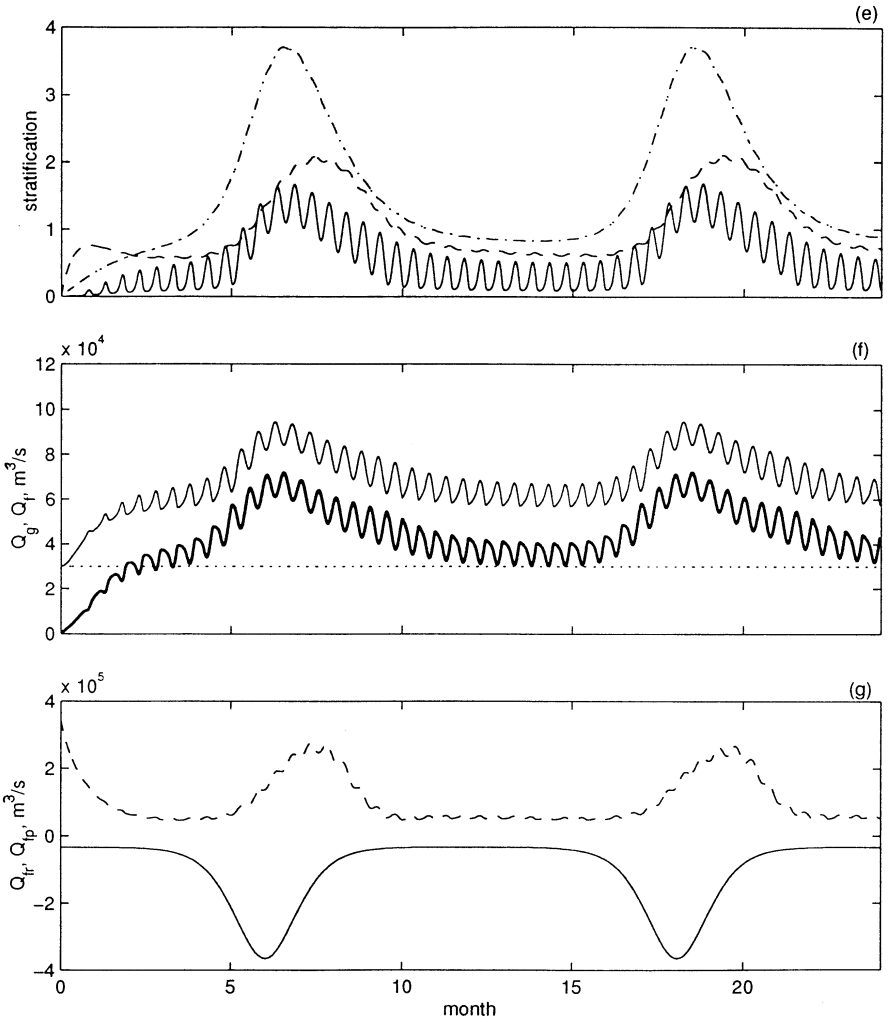

Fig. 3 *(Concluded)*

$$Q_r = Q_{rw} + Q_{rs}\ \mathrm{sech}^2\left[10\frac{\tilde{t} - \tilde{T}/2}{\tilde{T}}\right] \tag{1}$$

where Q_{rw} is the low runoff in winter and $Q_{rw} + Q_{rs}$ is the peak runoff at summer freshet. The period $\tilde{T}$ is one year. We choose a hyperbolic function to represent a pronounced peak discharge in summer (Fig. 3a). A fresh water flux Q_r is equivalent to a salinity forcing of $-Q_r S_0$ where S_0 is a reference salinity (Gill, 1982).

In the box model, the vertical mixing between the upper and lower boxes of Haro Strait is represented by a vertical mixing velocity ω_h, so that the volume of

water exchanged per unit time is $\omega_h A_h$. Because the spring-neap tidal cycle causes a fortnightly cycle in vertical mixing, we assume that ω_h varies with a period of $\tilde{T}/24$, i.e.,

$$\omega_h = \frac{1}{2}\omega_h^m f(\tilde{S}_{hl} - \tilde{S}_{hu}) \left(1 + \sin \frac{2\pi \tilde{t}}{\tilde{T}/24}\right) \tag{2}$$

where ω_h^m is the maximum mixing velocity at spring tides. It is assumed that no tidal mixing occurs during neap tides. We examined the salinity (and density σ_t) distributions in the Georgia-Fuca estuary at monthly intervals (Crean and Ages, 1971) and found that stratification in Haro Strait may be suppressed when there is strong stratification. We account for the effect of stratification by introducing $f(\tilde{S}_{hl} - \tilde{S}_{hu})$ in (2) and assuming

$$f = \frac{\Delta \tilde{S}_c}{\tilde{S}_{hl} - \tilde{S}_{hu}} \tag{3}$$

when $(\tilde{S}_{hl} - \tilde{S}_{hu}) \geqslant \Delta \tilde{S}_c$ and $f = 1$ when $\tilde{S}_{hl} - \tilde{S}_{hu} < \Delta \tilde{S}_c$. The tidal mixing is thus reduced when the stratification in Haro Strait exceeds a threshold. A corresponding vertical eddy diffusivity is $\kappa_{vh} = \omega_h h_u$ and its maximum at spring tides is denoted as κ_{vh}^m. To represent the weaker vertical mixing in Georgia and Fuca basins, we use vertical velocities ω_g and ω_f respectively. For simplicity, we assume both ω_g and ω_f to be constant. The corresponding eddy diffusivities are $\kappa_{vg} = \omega_g h_u$ and $\kappa_{vf} = \omega_f h_u$.

The western end of Juan de Fuca Strait shows a two-layer exchange with the Pacific, by which the upper Fuca box loses an amount of less saline surface water to the Pacific ocean while the lower box receives a slightly less amount of more saline deep water. From late spring to early fall, winds from the north to northwest produce upwelling of high salinity water over the shelf. From late fall to early spring, winds from the southeast favour coastal downwelling and low salinities. Thus the salinity of the water mass that is being transported eastward in the lower layer of Juan de Fuca Strait will depend on the timing, duration and intensity of the upwelling-downwelling processes over the shelf. We prescribe a seasonal variation of the Pacific salinity to be

$$\tilde{S}_p = 33 + \mathrm{sech}^2 \left[10 \frac{(\tilde{t} - \tilde{T}/2 - \tilde{t}_l)}{\tilde{T}}\right] \tag{4}$$

where $\tilde{t}_l = 2$ months. The Pacific salinity reaches a maximum of 34 in August when upwelling is most vigorous and falls to a minimum of 33 in winter, as shown in Fig. 3b. We use the hyperbolic function to simulate an intense but relatively short summer upwelling season. To account for the two-layer exchange flow, we allow for the horizontal advection of water mass between the Juan de Fuca Strait and Pacific Ocean, i.e., brackish water is exported from the upper box while saline

water is imported into the lower box. As an outer boundary condition on salinity, we relax the lower-layer salinity $\tilde{S}_{fl}$ to the Pacific salinity $\tilde{S}_p$ with a timescale t_r.

Water in the upper box of the Georgia basin is diluted by the fresh water input from the Fraser River. The resulting horizontal density difference (or pressure difference) between the Georgia and Haro upper boxes drives a horizontal flow between the two boxes. Similarly, when fresh water from Georgia Strait is pumped into Haro Strait, water in Haro Strait becomes diluted and the density difference between Haro and Juan de Fuca Straits generates a secondary estuarine circulation. We parametrize this gravitational estuarine circulation using the parametrization of Stommel (1961). If ρ_{gu}, ρ_{hu} and ρ_{fu} are the densities of the waters in the upper boxes of the Georgia, Haro and Fuca basins, then the volume flux of water between the Georgia and Haro basins $Q_g \propto (\rho_{hu} - \rho_{gu})$ and that between the Haro and Fuca basins $Q_f \propto (\rho_{fu} - \rho_{hu})$. Since stratification in the estuary is dominated by salinity differences, temperature is taken as constant. Using Stommels's parametrization, we obtain

$$Q_g = c_g(\rho_{hu} - \rho_{gu}) = c_g \beta \rho_0 (\tilde{S}_{hu} - \tilde{S}_{gu}), \tag{5}$$

$$Q_f = c_f(\rho_{fu} - \rho_{hu}) = c_f \beta \rho_0 (\tilde{S}_{fu} - \tilde{S}_{hu}), \tag{6}$$

in which c_g and c_f are two constants of proportionality, ρ_0 a reference density and β the saline contraction coefficient.

Consideration of the salt budgets in each box leads to

$$V_{gu}\frac{d\tilde{S}_{gu}}{d\tilde{t}} = Q_g(\tilde{S}_{gl} - \tilde{S}_{gu}) + \omega_g A_g(\tilde{S}_{gl} - \tilde{S}_{gu}) - Q_f S_0, \tag{7}$$

$$V_{gl}\frac{d\tilde{S}_{gl}}{d\tilde{t}} = Q_g(\tilde{S}_{hl} - \tilde{S}_{gl}) - \omega_g A_g(\tilde{S}_{gl} - \tilde{S}_{gu}), \tag{8}$$

$$V_{hu}\frac{d\tilde{S}_{hu}}{d\tilde{t}} = Q_g(\tilde{S}_{gu} - \tilde{S}_{hu}) + Q_f(\tilde{S}_{hl} - \tilde{S}_{hu}) + \omega_h A_h(\tilde{S}_{hl} - \tilde{S}_{hu}), \tag{9}$$

$$V_{hl}\frac{d\tilde{S}_{hl}}{d\tilde{t}} = Q_g(\tilde{S}_{hu} - \tilde{S}_{hl}) + Q_f(\tilde{S}_{fl} - \tilde{S}_{hl}) - \omega_h A_h(\tilde{S}_{hl} - \tilde{S}_{hu}), \tag{10}$$

$$V_{fu}\frac{d\tilde{S}_{fu}}{d\tilde{t}} = Q_f(\tilde{S}_{hu} - \tilde{S}_{fu}) + \omega_f A_f(\tilde{S}_{fl} - \tilde{S}_{fu}), \tag{11}$$

$$V_{fl}\frac{d\tilde{S}_{fl}}{d\tilde{t}} = Q_f(\tilde{S}_p - \tilde{S}_{fl}) - \omega_f A_f(\tilde{S}_{fl} - \tilde{S}_{fu}) + \frac{1}{t_r}V_{fl}(\tilde{S}_p - \tilde{S}_{fl}) \tag{12}$$

Nondimensionalizing salinities by S_0 and time by $t_s = V_{gu}/(c_g \rho_0 \beta S_0)$, we obtain

$$\frac{dS_{gu}}{dt} = q_g(S_{gl} - S_{gu}) + R_2(S_{gl} - S_{gu}) - F_1(t), \tag{13}$$

$$\frac{dS_{gl}}{dt} = \lambda_d\{q_g(S_{hl} - S_{gl}) - R_2(S_{gl} - S_{gu})\}, \tag{14}$$

$$\frac{dS_{hu}}{dt} = \frac{1}{\lambda_{hg}}\{q_g(S_{gu} - S_{hu}) + R_3 q_f(S_{hl} - S_{hu}) + R_4(S_{hl} - S_{hu})\}, \tag{15}$$

$$\frac{dS_{hl}}{dt} = \frac{\lambda_d}{\lambda_{hg}}\{q_g(S_{hu} - S_{hl}) + R_3 q_f(S_{fl} - S_{hl}) - R_4(S_{hl} - S_{hu})\}, \tag{16}$$

$$\frac{dS_{fu}}{dt} = \frac{\lambda_{hf}}{\lambda_{hg}}\{R_3 q_f(S_{hu} - S_{fu}) + R_5(S_{fl} - S_{fu})\}, \tag{17}$$

$$\frac{dS_{fl}}{dt} = \frac{\lambda_{hf}\lambda_d}{\lambda_{hg}}\{R_3 q_f(S_p - S_{fl}) - R_5(S_{fl} - S_{fu})\} + R_6(S_p - S_{fl}) \tag{18}$$

where the parameters are

$$\lambda_d = h_u/h_l = 1/3, \lambda_{hg} = V_h/V_g = 1/8, \lambda_{hf} = V_h/V_f = 1/4, \tag{19}$$

$$F_1(t) = R_{1w} + R_1 \text{ sech}^2\left[10\frac{(t - T/2)}{T}\right], R_{1w} = \frac{Q_{rw}}{c_g \rho_0 \beta S_0}, R_1 = \frac{Q_{rs}}{c_g \rho_0 \beta S_0}, \tag{20}$$

$$R_2 = \frac{\omega_g A_g}{c_g \rho_0 \beta S_0}, \tag{21}$$

$$R_3 = \frac{c_f}{c_g}, \tag{22}$$

$$R_4 = \frac{\omega_h A_h}{c_g \rho_0 \beta S_0} = \frac{1}{2} R_4^m f(S_{hl} - S_{hu})\left(1 + \sin\frac{2\pi t}{T/24}\right), R_4^m = \frac{\omega_h^m A_h}{c_g \rho_0 \beta S_0}, \tag{23}$$

$$R_5 = \frac{\omega_f A_f}{c_g \rho_0 \beta S_0}, \tag{24}$$

$$R_6 = t_r/t_s. \tag{25}$$

Here $S_{gu}, S_{gl}, S_{hu}, S_{hl}, S_{fu}, S_{fl}$ are nondimensionalized salinities. The nondimensionalized volumes fluxes are accordingly given by

$$q_g = S_{hu} - S_{gu}, \tag{26}$$

$$q_f = S_{fu} - S_{hu}, \tag{27}$$

There are six dimensionless parameters. If the salinity in the upper box of Georgia basin is 0 (fresh water) and that in the upper box of Haro Strait is S_0, then the volume flux from Georgia to Haro boxes is $c_g \rho_0 \beta S_0$. Thus $c_g \rho_0 \beta S_0$ represents the water mass transport driven by the largest possible salinity difference. Since the observed volume fluxes through the Juan de Fuca Strait are of order 10^5 m^3 s^{-1}, we choose $c_g \rho_0 \beta S_0 = 10^6$ m^3 s^{-1}. F_1 is the ratio of the fresh water flux to this water mass transport rate. $R_3 = c_f / c_g$ is a ratio of two proportional constants used in the Stommel parametrization. These constants are conversion factors from salinity (density) difference to volume fluxes and may be chosen to describe the specific conditions presented at the intersection between two boxes. For now, we assume $R_3 = 1$. The three parameters R_2, R_4 and R_5 are ratios of rates of water mass exchange due to vertical mixing to the water mass transport due to density difference. R_6 is the ratio of the estuarine timescale t_s to the relaxation timescale t_r for the lower box of the Juan de Fuca Strait. The nondimensional timescale $t_s = V_{gu}/(c_g \rho_0 \beta S_0) = 2 \times 10^5\ s \approx 2.3$ d. Thus a year is about 150 nondimensional time units, i.e., $T \approx 150$.

3 Seasonal cycle of estuarine circulation

The salinity equations (13) to (18) are solved numerically using a fifth-order Runge-Kutta method with adaptive time stepping (MATLAB Simulink). We start from a homogeneous salinity distribution, i.e., $\tilde{S}_{gu} = \tilde{S}_{gl} = \tilde{S}_{hu} = \tilde{S}_{hl} = \tilde{S}_{fu} = \tilde{S}_{fl} = 31$ at $t = 0$, but sensitivity studies suggest that annual cycles of estuarine circulation are independent of initial conditions. We choose the reference salinity S_0 to be the annual mean, $\tilde{S}_{pm} = 33.5$, of the Pacific salinity $\tilde{S}_p$.

To simulate a typical seasonal cycle, we use a winter runoff $Q_{rw} = 10^3$ m^3 s^{-1} and a summer peak discharge $Q_{rs} = 10^4$ m^3 s^{-1}, such that $R_{1w} = 0.001$ and $R_1 = 0.01$ (Fig. 3a). The Pacific salinity peaks two months later (Fig. 3b). LeBlond et al. (1994) suggested a vertical mixing velocity up to $\omega_h^m = 0.015$ m s^{-1} for Haro Strait. Using $A_h = 500$ km^2, we obtain $R_4^m = 0.5$ and a corresponding maximum eddy diffusivity $\kappa_{vh}^m = 5 \times 10^{-2}$ m^2 s^{-1}. We choose the threshold stratification $\Delta \tilde{S}_c = 0.2$. The spring-neap tidal cycle of eddy diffusivity in Haro Strait, modulated by the stratification effect, is shown in Fig. 3c. Tidal mixing is much reduced during summer freshet when strong stratification develops in Haro Strait. Mixing in Juan de Fuca Strait is weaker than in Haro Strait, so we choose $R_4 = 0.05$. This corresponds to an eddy diffusivity $\kappa_{vf} = 1.25 \times 10^{-3}$ m^2 s^{-1}. For the Strait of Georgia where mixing is weakest, we choose $R_2 = 0.01$ and an eddy diffusivity of 1.25×10^{-4} m^2 s^{-1}. Vertical mixing supplies fresh water to the deep layer of Georgia basin and is required in order to obtain a realistic prediction of $\tilde{S}_{gl}$.

If the relaxation term were the only term present on the right hand of (18) and S_p is constant, we obtain a solution given as

$$S_{fl} = S_p - [S_p - S_{fl}(0)]\mathrm{e}^{-R_6 t}, \tag{28}$$

$$\text{or } \tilde{S}_{fl} = \tilde{S}_p - [\tilde{S}_p - \tilde{S}_{fl}(0)]\mathrm{e}^{-\tilde{t}/t_r} \tag{29}$$

in dimensional terms. Assuming a typical value of 2 for $[\tilde{S}_p - \tilde{S}_{fl}(0)]$, the difference $[\tilde{S}_p - \tilde{S}_{fl}]$ will be reduced to less than 0.1 at $\tilde{t} \approx 3t_r$. If we require $\tilde{S}_{fl}$ be relaxed to $\tilde{S}_p$ in a month, we should choose $t_r = 10.2$ days or $R_6 = t_s/t_r = 0.23$. The relaxation time t_r is a measure of the response time taken for the deep Juan de Fuca water to equilibrate its salinity to the Pacific salinity. Because the Pacific salinity $\tilde{S}_p$ varies over the seasonal scale, however, t_r cannot be chosen too long or $\tilde{S}_{fl}$ will lag far behind $\tilde{S}_p$. In the model run shown in Fig. 3, we choose $R_6 = 0.12$ or a relaxation time of 2 months.

Figure 3d shows the predicted time series of salinities for the first two years of a five-year simulation. There is a "spin-up" adjustment in the first year after which the model produces repeating annual cycles. As the Fraser River releases fresh water into the Strait of Georgia, water in the upper layer become diluted: $\tilde{S}_{gu}$ falls to a minimum of 27.1 in July, one month after the freshet. It rises in the autumn and reaches a maximum of 30.1 in the following March. Salinity $\tilde{S}_{gl}$ in the lower Georgia box averages about 30.8, with a small seasonal variation of 0.4. Salinities in Haro Strait show seasonal as well as tidal variations. Surface salinity $\tilde{S}_{hu}$ varies from 29.0 in July to 31.4 in winter. The seasonal fluctuation is about 5 times as large as the fortnightly tidal modulation of 0.4. The salinity $\tilde{S}_{fl}$ of deep water in Juan de Fuca Strait varies from a minimum of 32.8 in June to a maximum of 33.4 in September.

In Fig. 3e we plot the time series of vertical stratification (i.e., difference between lower and upper box salinities) in the three basins. Stratification is strongest in the Strait of Georgia and weakest in Haro Strait. Waters appear to be well mixed in Haro Strait during spring tides in the winter, but strong stratification during the summer freshet suppresses the tidal mixing. A maximum stratification of 1.7 is reached during a neap tide at the peak of freshet. The stratification in Juan de Fuca Strait reaches a maximum of 2.1 in summer, but reduces to a minimum of about 0.6.

These model predictions of salinities are in reasonable agreement with observations. Griffin and LeBlond (1990) analyzed the salinity data from lighthouses in Active Pass at the entrance to Haro Strait and also at Race Rocks at the eastern end of the Juan de Fuca Strait. The amplitude of tidal fluctuation is 0.38 for the lighthouse station at Race Rocks, which compares with 0.4 for $\tilde{S}_{hu}$ produced from the model. For Juan de Fuca Strait, they reported a mean surface-layer salinity of $\tilde{S}_{fu} = 31$. The deep water salinity $\tilde{S}_{fl}$ varied between 33 and 33.5 over a year. Based on data collected on monthly cruises during the year of 1968, Crean and Ages (1971) produced contours of salinity distribution in the Georgia-Fuca basin. Using their salinity data, we have obtained estimates of box-averaged salinities in each of the six boxes, as shown in Fig. 4a. We divide the estuary into the Georgia, Haro and Fuca basins. The upper boxes occupy the top 50-m depth while the lower boxes extend from the 50-m depth to the ocean bottom. It is a subjective process to estimate the volume (or area) averaged salinities from measurements at a

limited number of points, particularly in Haro Strait where sampling stations were relatively sparse. We choose the algebraic mean of all salinities in a box as the box-averaged salinity. (It may be more appropriate to define an area of influence for each sampling station and use different weight functions for sampling points at different depths, but their choices must also be subjective.) Figures 4a and b show a general consistency between the modelled and observed annual cycle of salinities. Crean and Ages (1971) observed a rather constant salinity of 30.5 for the deep water in the Strait of Georgia, which is close to the model average of 30.8. The observations at monthly intervals could not resolve the spring-neap tidal cycle in the Haro Strait salinities, but the data showed that the stratification in this strait is significantly stronger in the summer than in the winter as shown in the model. The two salinities, $\tilde{S}_{gu}$ and $\tilde{S}_{fl}$, are directly forced by external forcing functions and their predictions could be improved if the model were forced by the observed values of Fraser River runoff and Pacific salinity for the year of 1968 rather than the representative values used in Fig. 3.

The two volume fluxes Q_g and Q_f predicted by the model are of comparable magnitude, reaching maxima of about (7.2 and 6.5) $\times$ 10^4 m^3 s^{-1} in June (Fig. 3f). It is noted that the tidal fluctuation components of Q_g and Q_f are out of phase. During spring tides strong mixing in Haro Strait increases the surface layer salinity, leading to increased water mass transport from the Strait of Georgia into Haro Strait but decreasing transport from Haro Strait out to the Juan de Fuca Strait, and vice versa during neap tides. Although Q_r varies by an order of magnitude over a year, Q_g and Q_f only change by a factor of 2 (see Fig. 3f), resulting in high values of Q_g/Q_r and Q_f/Q_r in low runoff months. The mean ratios of the volume fluxes to the river runoff, Q_g/Q_r and Q_f/Q_r, are about 25. Due to mixing and entrainment, estuarine volume fluxes are much greater than the river runoff. Based on current meter measurements, the inflow and outflow volume fluxes in the Juan de Fuca Strait were estimated to be in the range of (9 to 16) $\times$ 10^4 m^3 s^{-1} (Thomson, 1981). Using a three-dimensional baroclinic model, Masson and Cummins (1999) estimated a volume flux of about 9×10^4 m^3 s^{-1} during May. These are somewhat larger than our model values. The measured volume fluxes through the Juan de Fuca Strait presumably also include contributions from smaller runoffs such as from the Skagit River (in the Puget Sound drainage basin to the south) which are not considered in this box model. If repeating annual cycles of salinities are to be produced, the total salt budget for the estuary must be conserved. The negative salinity flux due to Fraser River runoff is $Q_{fr} = -Q_r \tilde{S}_{pm}$. The total rate of salt exchange between the Juan de Fuca Strait and Pacific Ocean consists of an advective part and an apparent flux due to relaxation, i.e.,

$$Q_{fp} = Q_f(\tilde{S}_p - \tilde{S}_{fu}) + \frac{\lambda_{hg}}{\lambda_{hf}\lambda_d} R_6(c_g \rho S_0 \beta)(\tilde{S}_p - \tilde{S}_{fl}). \tag{30}$$

To close the salt budget, the annual integral of Q_{fp} must balance that of Q_{fr}. Sensitivity studies show that the salt budget can be conserved for $3t_r$ ranging from

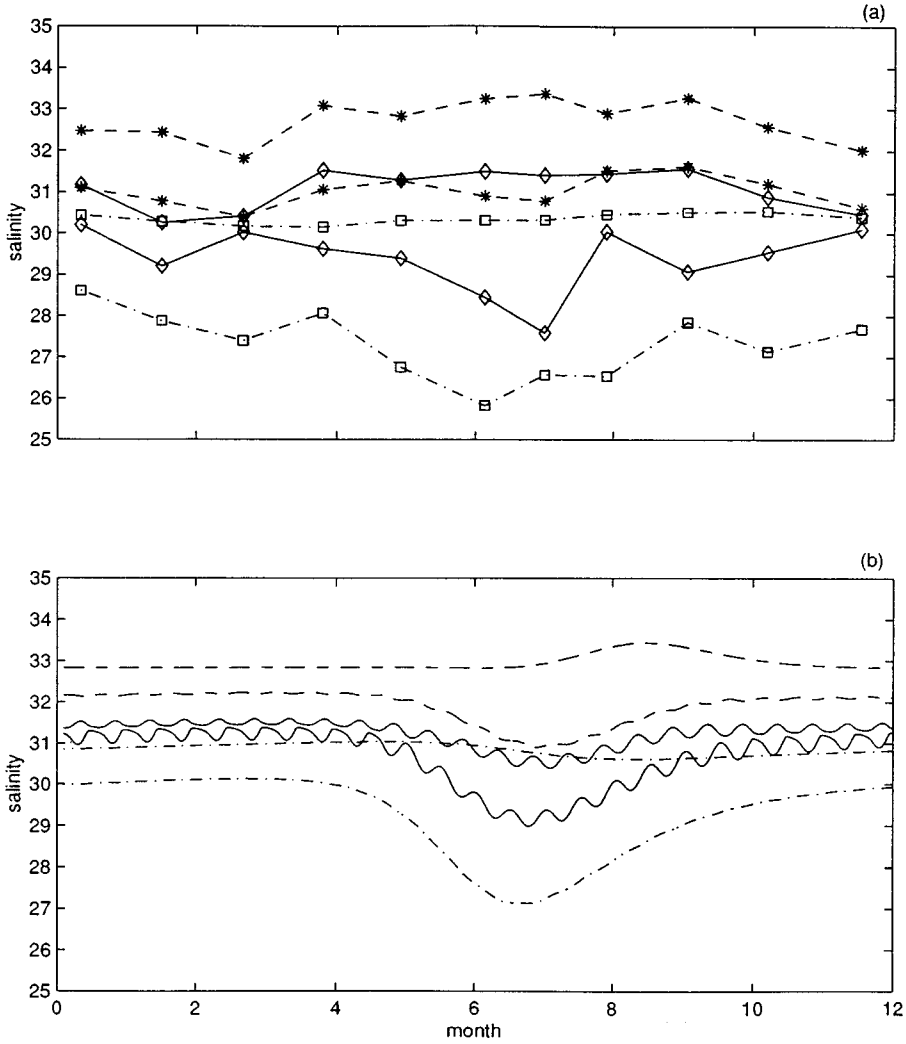

Fig. 4 Comparison between the box-averaged salinities estimated from Crean and Ages (1971) observations (a) and those from the numerical model (b) (reproduced from Fig. 3d). Dot-dashed lines (square points) represent salinities in Georgia basin, solid lines (diamond points) in Haro Strait and dashed lines (star points) in Fuca basin.

one to six months, although a relaxation time of 2 months gives the best fit for the seasonal cycle of salinities in the Juan de Fuca Strait. As shown in Fig. 3g, over a year the negative salinity flux Q_{fr} resulting from the Fraser River runoff is balanced by the positive salinity flux Q_{fp} coming from the Pacific Ocean to Juan de Fuca Strait. The annual integral of $Q_{fp} + Q_{fr}$ is less than 1% of $\int_0^{\tilde{T}} (-Q_r \tilde{S}_{pm}) d\tilde{t}$.

4 Interannual variability driven by variations in Fraser River runoff and in shelf water properties

Historical records show that the Fraser River runoff varies from year to year (Thomson, 1981). This interannual variability in runoff is related to the varying amounts of snow deposition in the mountains of British Columbia that are carried by the winter storms from the Pacific Ocean (Cayan and Peterson, 1989). Examination of time series and horizontal patterns of Sea Surface Temperature (SST) and Sea Level Pressure (SLP) in the North Pacific revealed a possible regime shift from 1976 to 1977 (Wallace and Gutzler, 1981; Nitta and Yamada, 1989). Before the shift, the Aleutian Low pressure centre was displaced westward and surrounded by a weak SLP gradient. In this regime the Gulf of Alaska is stormier, resulting in increased snow accumulation and runoff in British Columbia. After the regime shift, the Aleutian Low moves eastward and storm winds become less frequent, therefore smaller amounts of fresh water are available for the Georgia-Fuca estuary. Analysis of longer time series shows that several such interdecadal shifts may have occurred in this century (Zhang et al., 1997).

The interdecadal change accounts for a significant part of the variability observed in the Fraser River runoff. The amplitude of decadal variation is about 40% of the standard deviation in the annual-averaged runoffs (Ebbesmeyer et al., 1989). The decadal variability may also affect coastal water properties. For example, time-mean SST was higher after 1977 over the tropical Pacific and off the west coast of the Americas.

To mimic a possible regime shift from high to low runoff, we performed a numerical experiment in which the peak Fraser River runoff at the summer freshet suddenly shifts, in year 5, to a level half that of the normal value (Fig. 5). Figure 5a shows the fresh water and salinity fluxes, which remain approximately balanced over each year. Figures 5b and 5c show the time series of the salinities and volume fluxes. The estuarine circulation responds rapidly to the change in fresh water flux and adjusts to the new runoff within a year. The same short response time is obtained when there is a sudden increase in the Fraser River runoff. There are debates about whether the Pacific Ocean climate changes in the 70s are abrupt or more gradual. We have examined the cumulative effect of several years of low river runoffs by decreasing the peak runoff at small increments for five years and then gradually returning it to the normal level. Once again, the estuarine circulation shows a rapid response. Model runs with successive years of high runoffs yield the same result.

Although the Fraser River runoff correlates with the climate indices of the North Pacific on decadal timescales, it shows considerable interannual variability (Ebbesmeyer et al., 1989). To account for this, we use a stochastic function to represent Q_r in which the peak runoff, the start-time and duration of the freshet vary randomly within observed ranges, as shown in Fig. 6a. The salinity of the water which enters the deep layer of the Juan de Fuca Strait shows a negative but relatively low correlation with the North Pacific climate indices (Ebbesmeyer

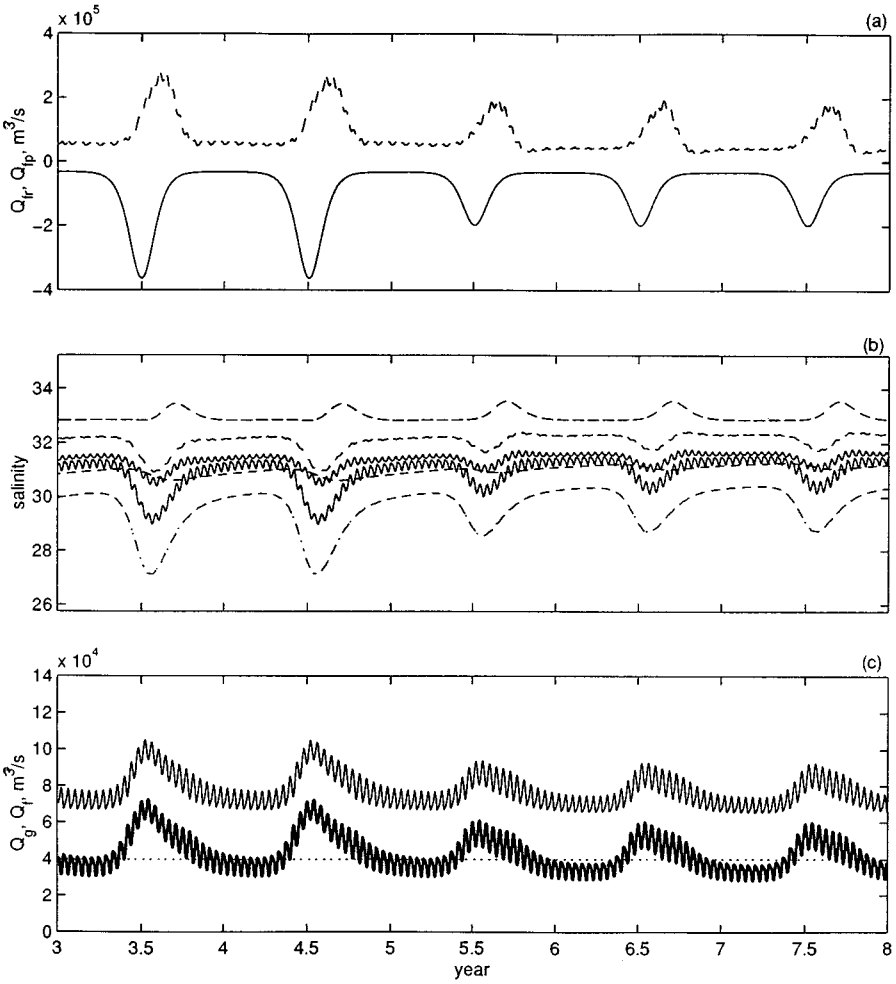

Fig. 5 Response of estuarine circulation to an abrupt decrease in the Fraser River runoff. (a) Salinities fluxes Q_{fr} (solid) and Q_{fp} (dashed), (b) salinities and (c) volume fluxes. Same convention for the line types as in Fig. 3 with Q_f offset by 4 units.

et al., 1989). To consider possible interannual variability in the properties of the continental shelf water, we also use a stochastic function to represent S_p (see Fig. 6b). Figure 6c shows the model results forced by stochastic fluctuations of Q_r and S_p. $\tilde{S}_{gu}$ and $\tilde{S}_{hl}$ closely track the forcing functions. The salinities in the other boxes also adjust rapidly to the changes. During year 2, salinities in the deep boxes show a progressive decrease from Juan de Fuca Strait to the Strait of Georgia, i.e., $\tilde{S}_{fl} \geqslant \tilde{S}_{hl} \geqslant \tilde{S}_{gl}$, in agreement with the Crean and Ages (1971) observations. During the summer in year 5, however, water in the deep layer of the Strait of Georgia

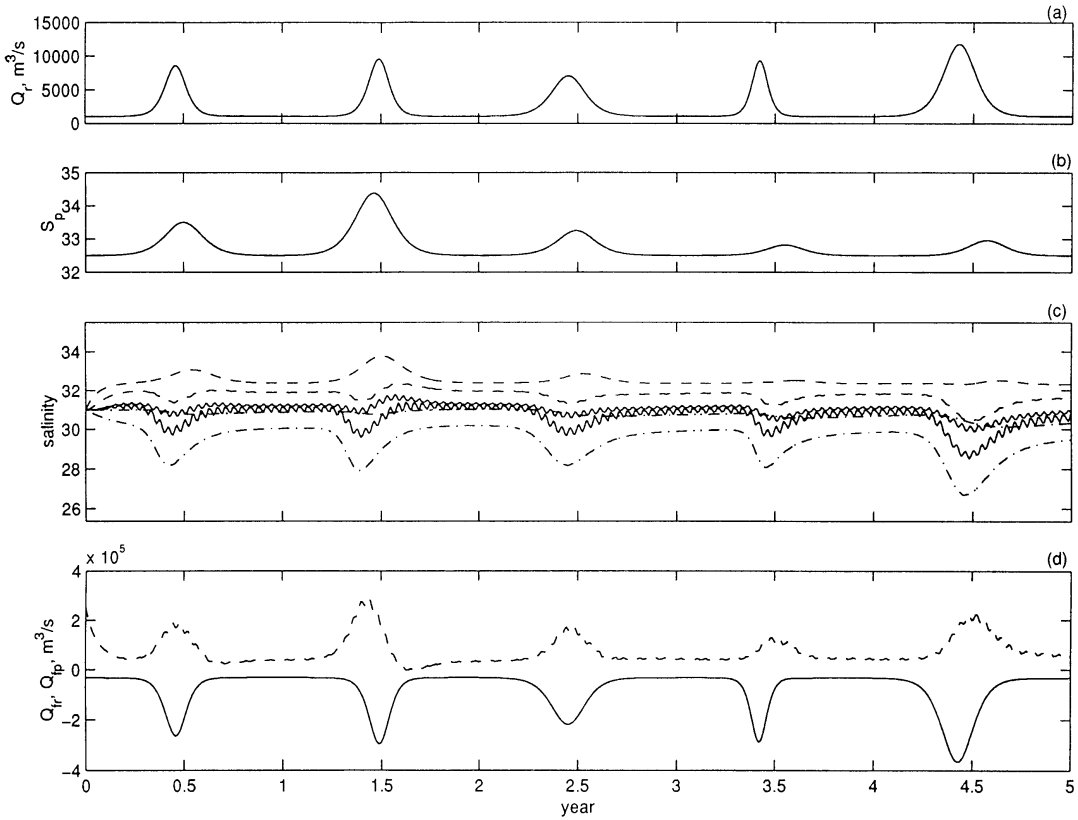

Fig. 6 Response of estuarine circulation to stochastic changes in the Fraser River runoff and in the salinity of the continental shelf water. (a) Fraser River runoff Q_r, (b) Pacific salinity S_p, (c) salinities and (d) salinities fluxes Q_{fr} (solid) and Q_{fp} (dashed). Same convention for the line types as in Fig. 3.

becomes saltier than its counterpart in Haro Strait. The precise ordering of the deep water salinities appears to depend on the phase lag between the freshet and coastal upwelling as well as the magnitudes of the runoff and the shelf salinity fluctuation at a particular year.

In summary, it appears that interannual to interdecadal changes in the Fraser River runoff and in the shelf water properties will be reflected quickly in the changes of the estuarine circulation and salinity stratification in the estuary. This result is consistent with the studies by Waldichuck (1957) and England et al. (1996) who show a short flushing time of about one year.

5 Conclusions

We have developed a six-box model for the Strait of Georgia and Juan de Fuca Strait in which the estuarine circulation is driven by Fraser River runoff but modulated by the spring-neap cycle of tidal mixing in Haro Strait. The model produces a reasonable prediction for the seasonal variations of salinities and volume fluxes. Multiple-year calculations show a rapid response of the estuarine circulation to the interannual changes of Fraser River runoff and the shelf water properties.

Satellite imagery shows that the prevailing summer northwesterly winds pile up the Fraser River plume in the southern Strait of Georgia and may thus enhance the transport of fresh water out to Haro Strait. It may be possible to modify the Stommel parametrization by allowing the proportionality constants to vary with the wind direction and magnitude. However, the marked seasonal cycle in the prevailing winds give rise to complex flow dynamics that are outside the scope of this box model. A fine-resolution three-dimensional baroclinic model, that includes the effects of variable river runoff and seasonal winds, has been developed at the Institute of Ocean Sciences (Masson and Cummins, 1999). This model resolves more physical processes such as coastal currents and deep return flow. However, it is beyond the current computing resources to run this kind of model over the many years which we need to understand long-term climate change in the physical properties of coastal basins, much less associated ecosystem changes. We believe that a combination of different modelling approaches will enable us to investigate coastal processes over a range of timescales.

Acknowledgements

We are grateful to Rich Pawlowicz for many helpful suggestions. We also thank Patrick Cummins, Dave Mackas, Diane Masson and Rick Thomson for interesting discussions. This work is supported by Canadian Department of Fisheries and Ocean High Priority Project funding.

References

CAYAN, D.R. and D.H. PETERSON. 1989. The influence of North Pacific atmospheric circulation on stream flow in the west. In: *Aspects of Climate Variability in the Pacific and the Western*

Americas. D.H. Peterson (Ed.), Geophysical Monograph, American Geophysical Union, Washington, D.C. pp. 375–397.

CREAN, P.B. and A. AGES. 1971. Oceanographic records from twelve cruises in the Strait of Georgia and Juan de Fuca Strait. Dept. Energy, Mines and Resources, Canada, 1, 55 pp.

———; T.S. MURTY and J.A. STRONACH. 1988. Mathematical modelling of the tides and estuarine circulation: The coastal seas of southern British Columbia and Washington State. In: *Lecture notes on Coastal and Estuarine Studies* 30, M.J. Bowman et al. (Eds.) Springer-Verlag, 471 pp.

EBBESMEYER, C.C.; C.A. COOMES, G.A. CANNON and D.E. BRETSCHNEIDER. 1989. Linkage of ocean and fjord dynamics at decadal period. In: *Aspects of Climate Variability in the Pacific and the Western Americas*. D.H. Peterson (Ed.), Geophysical Monograph. American Geophysical Union, Washington, D.C., pp. 399–417.

ENGLAND, L.A.; R.E. THOMSON and M.G.G. FOREMAN. 1996. Estimates of seasonal flushing times for the southern Georgia basin. Can. Tech. Rep. Hydrogr. Ocean Sci., 173, 24 pp.

FOREMAN, M.G.G.; R.A. WALTERS, R.F. HENRY, P. KELLER and A.G. DOLLING. 1994. A tidal model for eastern Juan de Fuca Strait and southern Strait of Georgia. *J. Geophys. Res.* **98(C2)**: 2509–2531.

GARGETT, A. and B. FERRON. 1996. The effects of differential vertical diffusion of *T* and *S* in a box model of thermohaline circulation. *J. Mar. Res.* **54**: 827–866.

GILL, A.E. 1982. *Atmosphere-Ocean Dynamics*. Academic Press, New York, 662 pp.

GRIFFIN, D.A. and P.H. LEBLOND. 1990. Estuary/ocean exchange controlled by spring-neap tidal mixing. *Estuar. Coastal Shelf Sci.* **30**: 275–297.

LEBLOND, P.H.; H. MA, F. DOHERTY and S. POND. 1991. Deep and intermediate water replacement in the Strait of Georgia. ATMOSPHERE-OCEAN, **29(2)**: 288–312.

———; D.A. GRIFFIN and R.E. THOMSON. 1994. Surface salinity variations in the Juan de Fuca Strait: test of a predictive model. *Cont. Shelf Res.* **14(1)**: 37–56.

MACKAS, D.L. and P.J. HARRISON. 1997. Nitrogenous nutrient sources and sinks in the Juan de Fuca Strait/Strait of Georgia/Puget Sound estuarine system: assessing the potential for eutrophication. *Estuar. Coastal Shelf Sci.* **44**: 1–21.

MASSON, D. and P. CUMMINS. 1999. Numerical simulations of a buoyancy-driven coastal countercurrent off Vancouver Island. *J. Phys. Oceanogr.* **29**: 418–435.

NITTA, T. and S. YAMADA. 1989. Recent warming of tropical sea surface temperature and its relationship to the Northern Hemisphere circulation. *J. Meteorol. Soc. Jpn.* **58**: 187–193.

OTT, M. and C. GARRETT. 1998. Frictional estuarine circulation in Juan de Fuca Strait, with implications for secondary circulation. *J. Geophys. Res.* **103(C8)**: 15657–15666.

STOMMEL, H. 1961. Thermohaline convection with stable regimes of flow. *Tellus*, **13**: 224–230.

THOMSON, R.E. 1981. Oceanography of the British Columbia coast. In: *Canadian Spec. Pub. Fish. Aquat. Sci.*, Vol. 56, 291 pp.

———. 1994. Physical oceanography of the Strait of Georgia-Puget Sound-Juan de Fuca Strait system. *In*: Rev. of the Marine Environment and Biota of Strait of Georgia, Puget Sound and Juan de Fuca Strait, Proc. BC/Washington Symposium on the Marine Environment, 13–14 Jan. 1994, Can. Tech. Rep. Fish. Aquatic Sci. No. 1948 pp. 36–100.

———; B.M. HICKEY and P.H. LEBLOND. 1989. The Vancouver Island Coastal Current: fisheries barrier and conduit. Effect of variability on recruitment and evaluation of parameters used in stock assessment models. *Canadian Spec. Pub. Fish. Aquat. Sci*, **108**: 265–296.

THUAL, O. and J.C. MCWILLIAMS. 1992. The catastrophe structure of thermohaline convection in a two-dimensional fluid model and a comparison with low-order box model. *Geophys. Astrophys. Fluid Dyn.* **64**: 67–95.

WALDICHUCK, M. 1957. Physical oceanography of the Strait of Georgia, British Columbia, *J. Fish. Res. Board Canada*, **14**: 321–486.

WALLACE, J.M. and D.S. GUTZLER. 1981. Teleconnections in the geopotential height field during the Northern Hemisphere winter. *Mon. Weather Rev.* **109**: 784–812.

YZHANG, Y.; J.M. WALLACE and D.S. BATTISTI. 1997. ENSO-like interdecadal variability: 1900–93. *J. Clim.* **10(5)**: 1004–1020.